Ring−Polymer Dynamics in Gels: Supercoiled and Relaxed Circular DNA in Polyacrylamide

Björn Åkerman†

Department of Physical Chemistry, Chalmers University of Technology, S-412 96 Göteborg, Sweden

Received: April 17, 1998; In Final Form: August 10, 1998

Velocity and orientation measurements have been used to study the electrophoretic (1.9−22.5 V/cm) and Brownian motion of supercoiled and relaxed circular DNA (2926 and 5386 base pairs) in polyacrylamide gels (5% T, 3.3% C), using as controls linear molecules of either the same contour length or the same radius-of-gyration. Circular DNA deviate from the cyclic reptation of the linear counterparts but in a different manner at high and low field strengths because the circles tend to visit different substructures of the heterogeneous polyacrylamide gel at low and high fields. At 22.5 V/cm circles are first (within 15 ms) weakly aligned with the field by migration, before slowly (over a period of tens of seconds) becoming immobilized by impalement on protruding gel-fibers, which lead to a strongly enhanced field alignment. The rate of field-free decay for the parallel orientation is similar to that in free solution (time constants 20−40 ms, depending on DNA size), which shows that impalement occurs mainly in the more open parts of the gel. At 1.9 V/cm the circles migrate slowly and in wide zones compared to the linear form. Unexpectedly, the circles are oriented perpendicularly to the field direction, in a weak and slow manner (rise time, 50 s). The perpendicular orientation decays about 1000 times more slowly than the impalement-induced parallel orientation and furthermore is not observed in comparative experiments in agarose gels (which the paralell orientation mode is). The perpendicular mode is ascribed to a temporary squeezing of the circles against the bottom of "lobster traps" between dense regions of the polyacrylamide gel, which can be penetrated by the linear molecules but not by the circles due to DNA bending stiffness. At intermediate field strengths impaled and lobster-trapped circles exist side-by-side, as evidenced by the concomitant observation of both orientation modes. Data on the shortest pulses which detrap impaled molecules in intermittent and reversed fields, respectively, are combined to estimate the diffusion constant of circular DNA for translation off the gel fibers.

Introduction

The process of DNA motion in gels is a subject of broad interest. Electrophoretic migration in porous media gels is an important technique for analysis and preparation of DNA molecules of different sizes. DNA in gels may also be used as model systems for polymer dynamics in restricted environments, such as concentrated polymer solutions used in capillary electrophoresis[1] and the congested interior of the biological cell. So far most of the experimental and theoretical work on DNA in gels has dealt with linear molecules, and a good understanding of their electrophoretic migration and separation has been obtained.[2−4] Most studies have concentrated on long DNA, which basically migrate in an end-on fashion referred to as reptation. However, since the DNA polymer coils become wrapped and stretched around gel fibers and subsequently slide and contract back into the coiled state, the reptation is modulated by a cyclic extension and contraction of the molecules during the migration.[4,5]

Circular molecules in gels have received comparatively little attention in spite of the fact that these DNA forms are biologically important and furthermore usually are separated from their linear counterparts by electrophoresis in gels. Circular molecules are also of theoretical interest since they cannot reptate in the sense of a linear molecule. Linear DNA tend to move end-on, i.e., along an imaginary tube (Figure 1), because in order to move laterally it has to overcome the energy barrier[6,7] associated with the formation of loops of DNA between gel fibers. A circular molecule, on the other hand, always has to overcome the loop barrier in order to move as shown in (Figure 1). The nature of such loop barriers is of fundamental

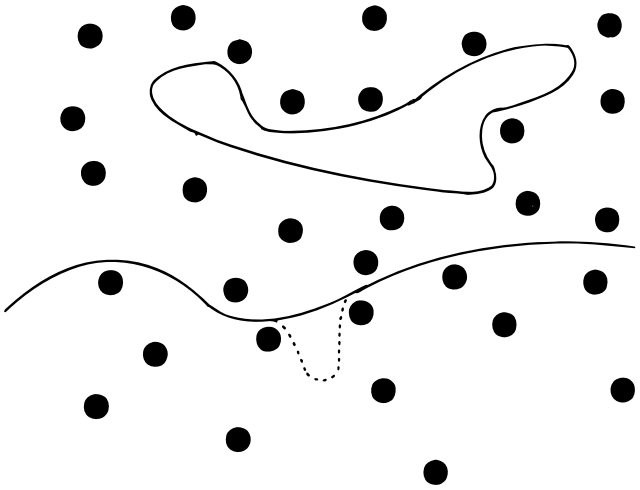

Figure 1. Relaxed circular and reptating linear DNA in a gel. For the linear molecule the dashed curve shows the process of loop formation, which is compulsory for the circular form.

† Phone: 46317723052. Fax: 46317723858. E-mail: baa@phc.chalmers.se.

10.1021/jp981905q CCC: $15.00
Published on Web 10/10/1998

importance for polymer dynamics in restricted geometries,[8] and circular polymers are one way of studying them. For both entropic and enthalpic reasons, such barriers exist if the distance between obstacles is comparable to the persistence length of the polymer,[6−8] which for example is the case for double-stranded DNA in agarose gels.[7,9]

Mobility studies have indeed revealed a specific behavior of circular DNA in agarose gels, in terms of an electrophoretic arrest which does not occur for linear DNA.[10−12] Impalement on protruding gel fibers has been suggested on the basis of effects of DNA size[12] and reversed fields,[13] and this proposal has found strong support in measurements of the electrophoretic orientation.[13] The circular molecules lack an overshoot in the orientation response, because, being impaled, they cannot slide around the gel fiber and contract, which is the process behind[14] the oscillatory orientation response observed with the linear form.[15] Finally, the degree of orientation is considerably higher because an impaled circle will be more efficiently stretched than the linear form, which is only transiently anchored by wrapping.

Theoretical studies of the Brownian[16] and electrophoretic[17] motion of circular DNA under the topological constraints of Figure 1 have been performed in regular lattices, but the effect of impalement has not been incorporated to date. In order to test those theories, we therefore turned to polyacrylamide gels, the idea being that impalement might be less severe than in agarose gels because slender and flexible polyacrylamide chains should be less efficient hooks than the thicker and stiffer agarose fibers. However, extensive studies of velocity and orientation in constant and pulsed fields[13] showed that also in polyacrylamide the circular DNA do become trapped reversibly by impalement on protruding obstacles.

This was the first demonstration of such defects in the polyacrylamide gel, which otherwise is fairly well-characterized and well-known for being strongly heterogeneous due to the free-radical nucleation of the polymerization. Dense regions forming around nucleation centers are surrounded by more open regions which result from the depletion of monomer. The result is a wide pore size distribution, where the dense regions have pore sizes as small as 20−90 Å,[18] whereas the open parts contain cavities which typically are 1000 Å in diameter.[19]

In the trapping study[13] an additional topological twist, so to speak, was added by exploiting the possibility of circular DNA to form supercoiled structures. It was shown that in both polyacrylamide and agarose gels a supercoiled species is less efficiently trapped than the corresponding relaxed form,[13] most probably because it is less prone to being impaled since the target area for the gel fibers is reduced by the crossing of the helix with itself. In agarose the supercoil is not trapped at all, whereas in polyacrylamide the probability for impalement is finite but 2−4 times lower than for the nicked species.[13] These observations were found to be consistent with the gel fibers being about 10 times thicker in agarose than in polyacrylamide.

Impalement requires that the field is strong enough to overcome escape by Brownian motion. Here we extend the earlier strong-field study[13] of the electrophoretic behavior of circular DNA in polyacrylamide gels to low and intermediate fields. As controls we use two sizes of linear DNA, one which has the same contour length and one with the same radius-of-gyration as the circles. This is important since either of these measures of DNA size can be determinants of the electrophoretic behavior in gels, at least in the case of linear DNA.[15] The radius-of-gyration is most important for small DNA, whereas the contour length becomes the relevant size parameter for the migration of large DNA,[4] with small and large being given by the ratio between the radius-of-gyration and the average pore radius.[15]

TABLE 1: Radii-of-Gyration (Å) of the Used DNA[a]

R_G (Å)	ΦX174	pIBI	1353 base pairs
linear	1700	1200	750
nicked circle	1200	840	not studied

[a] Calculated from wormlike chain model with persistence length of 500 Å and without excluded volume effects.

Here we show that also at low fields the behavior of the circles is different from that of linear molecules, but for a reason other than impalement. Indeed, the results support that the circles are subject to the topological constraints shown in Figure 1. The field-free relaxation of the electrophoretic orientation is also studied, and this is to our knowledge the first experimental study of the Brownian conformational dynamics of circular DNA in a gel. In addition data are presented that further clarify the impalement mechanism for circles and which support the cyclic reptation mechanism for the linear form.

Materials and Methods

DNA and Gel Samples. Polyacrylamide (Biorad) gels (5% T and 3.3% C), agarose (Biorad, DNA-grade) gels (1%) and hydroxyethylated agarose gels (Nusieve, FMC; 2%) were all formed at 20 °C. All experiments have been performed using native (nonstained) double-stranded DNA in TBE buffer (50 mM Tris, 50 mM borate, 1.25 mM EDTA, pH = 8.2). Supercoiled and nicked ΦX174 DNA (5386 base pairs) were from New England Biolabs. Supercoiled and nicked pIBI30 DNA (2926 base pairs) were from IBI. Linear pIBI30 was obtained by cleavage with EcoRI restriction endonuclease. A 1353 base pairs linear fragment was obtained from the HaeIII digest of ΦX174 (Pharmacia). The supercoiled samples contained about 5% nicked circles; the nicked samples, about 10% linear DNA. The superhelical densities[20] were −0.053 for pIBI and −0.061 for ΦX174,[13] which corresponds to 14 and 31 negative superhelical turns per molecule, respectively. Col1 plasmid DNA (10 900 base pairs) was from Sigma and contained 60% supercoil and 40% nicked circles. DNA concentrations were in the range 25−150 μM nucleotides, as determined by absorption at 260 nm, using the extinction coefficient 6600 M^{-1} cm^{-1}.

It should be noted that the relaxed circles are nicked, as opposed to covalently closed. Hagerman and co-workers[21] have shown that whereas removal of one base increases the flexibility of (linear) DNA substantially, a nick has little effect as monitored by electrophoresis in polyacrylamide gels (6% T).

Table 1 shows the radii-of-gyration[22] of the employed linear and relaxed circular DNA. At the present degrees of supercoiling the radius-of-gyration of supercoiled molecules can be expected to be about 20% lower than for the nicked circle.[20] The pIBI circles could thus be compared with linear molecules of either the same contour length (pIBI) or half the contour length but approximately the same radius-of-gyration (1353 base pairs), and the same holds for ΦX174.

Velocity. Slab gels were run in submarine mode, as described earlier.[13] In all velocity experiments a sharp starting zone about 2 mm into the gel was obtained by a 5 min prerun with field inversion gel electrophoresis ($T_+ = 1$ s; $T_- = 0.1$ s) at 22.5 V/cm. The electrophoretic velocity was calculated from the distance migrated relative to the starting position (which was determined on an identical but separately stained gel),[13] divided by the effective running T_{eff}. In constant field (CF) electro-

phoresis T_{eff} was equal to the actual running time T_{run}. In field inversion gel electrophoresis (FIGE), $T_{eff} = T_{run}(T_+ - T_-)/(T_+ + T_-)$; in intermittent field gel electrophoresis (IFGE), $T_{eff} = T_{run}(T_{on})/(T_{on} + T_{off})$.

Linear Dichroism. Electrophoretic orientation was measured in a vertical cell for linear dichroism (LD), as described earlier.[13,23] The DNA is introduced into the measuring position in the gel by FIGE, which separates the DNA forms, ensuring that measurements are performed on topologically pure samples. Each DNA type (size and topology) was studied in at least two different and freshly prepared gels. LD can be used to measure the average degree of DNA-helix orientation in terms of an orientation factor S which is related to the angle θ between the helix axis and the field direction.

$$S = \langle 3 \cos^2 \theta - 1 \rangle / 2 \quad (1)$$

If the preferred helix alignment is along the electric field, S is positive, whereas a negative S indicates a net orientation perpendicular to the field.[24] If all molecules are perfectly aligned with the field ($\theta = 0°$), S is equal to 1, and $S = -1/2$ if all molecules are oriented with their helix axis perpendicular to the field direction ($\theta = 90°$). Finally $S = 0$ if the helix axis orientation is random but will also result if there are concomitant parallel and perpendicular contributions of the same magnitude. S is obtained by dividing the LD by the isotropic absorption (A_{iso}) of the sample when the DNA molecules are randomly oriented (absence of field)[24]

$$LD/A_{iso} = -1.48S \quad (2)$$

The negative sign of the so-called optical factor, −1.48 in (2), reflects the perpendicular orientation of the transition moments with respect to the DNA helix axis.[25]

Results

Velocity. *Constant Fields*. The electrophoretic velocity reveals distinct differences in the behavior of circular and linear molecules in polyacrylamide gels. However, the circles deviate from the linear form in different ways at high and low fields. Figure 2a shows the results of a migration experiment at 22.5 V/cm, using two gels which were prepared and loaded in the same way. The gel to the right was taken out of the electrophoresis cell and stained after the prerun with inverted fields (see Material and Methods), in order to determine the starting position for the constant field experiment. The gel to the left was subjected to an additional 1 h of constant field electrophoresis before staining. The lack of motion of the bands shows that at this high field strength the circles are trapped at the starting position. The weak smear for the supercoiled form is due to its lower probability of trapping.[13] The fact that the linear form migrates (left gel) shows that trapping requires a circular topology. At the lower field strength of 3.8 V/cm (Figure 2b, where the linear DNA was run as a separate sample), the circles do migrate but slowly compared to the linear form and with much broader zones. The broad and slow zones cannot be caused by physical adsorption to the gel since it would be occurring also for the linear molecule. There is thus an interaction with the gel matrix which acts specifically to slow down the circles, but without forcing them to a complete stop. One of the topics in this study is whether the circle-specific retardation at low fields is related to the impalement effect which gives rise to circle immobilization in stronger fields.[13] Figure 2c summarizes the velocity data as a function of (constant) field strength. At low and intermediate fields the velocity increases

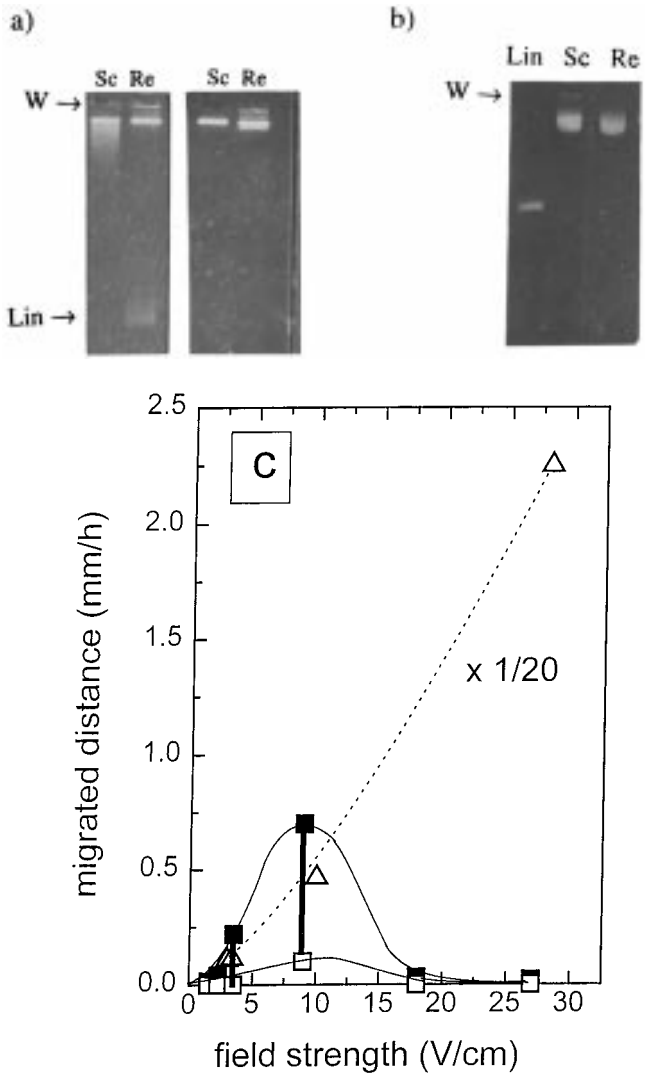

Figure 2. Constant field electrophoresis of supercoiled (Sc), nicked circular (Re), and linear (Lin) ΦX174 DNA (5386 base pairs) in 5% T polyacrylamide gel: (a) 22.5 V/cm (linear form is minor component in the relaxed sample), right gel after prerun with FIGE, left gel after additional 60 min of constant field; (b) 3.4 V/cm (linear form run in separate lane; *W* is position of well); (c) velocity vs field strength. Supercoiled and nicked circles (squares) comigrate as wide zones, where solid and open symbols represent approximate leading and trailing ends of zone. For the linear form (triangles) the symbol size represents the width of the zone.

with increasing field, but the zones are wide. At higher fields the velocity decreases with increasing field strengths and at high enough fields the molecules are immobilized.

Pulsed Fields. Velocity measurements in pulsed fields have proven useful in attempts to understand the migration process in strong fields.[13] Here we notice that in field inversion gel electrophoresis (FIGE) a graph of the displacement of linear and circular DNA vs time is linear and passes through the origin (Figure 3a). This constant velocity shows that also the circular molecules are capable of normal migration through the gel under appropriate conditions. This indicates that the wide zones for the circles in low constant fields (Figure 2b) are not just simply the result of an attempt to force these comparatively large DNA molecules through a too tight polyacrylamide gel. It is concluded that it is relevant to use these DNA sizes in polyacrylamide gels for studies of the effect of a porous network on the motion of circular molecules.

In the previous study impaled circles were detrapped by

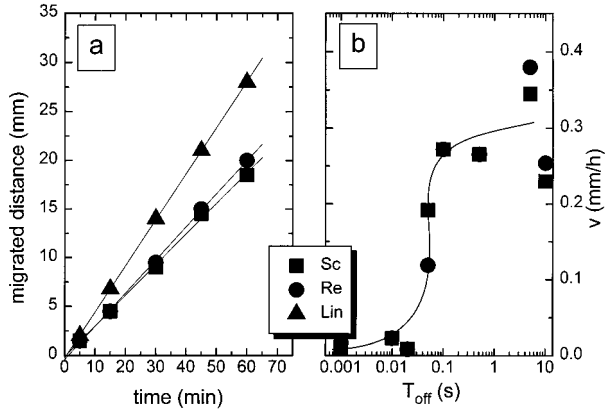

Figure 3. Pulsed field electrophoresis of supercoiled (Sc), nicked circular (Re), and linear (Lin) ΦX174 DNA in 5% T polyacrylamide gel at 22.5 V/cm: (a) migrated distance vs running time in field inversion electrophoresis ($T_+ = 1$ s; $T_- = 0.1$ s); (b) velocity vs T_{off} (duration of field-free period) in intermittent field electrophoresis ($T_{on} = 1$ s).

backward migration in a reversed field, and the required duration of the reversed pulse was used to calculate the depth of the trap.[13] Here we instead unhook the circles by diffusion by replacing the backward pulses by field-free pauses between the forward pulses (intermittent field electrophoresis). This allows us to study the Brownian motion of circles in gels. The effect of the duration of the pauses (T_{off}) was investigated by setting the duration of the on-pulse (T_{on}) at a fixed value of 1 s. This forward duration is known to trap the circles: in field-inversion experiments with 1 s forward pulses the net velocity was nonzero only if the backward pulses were long enough to unhook the molecules.[13] The effect of T_{off} in intermittent fields is similar, as shown in Figure 3b. The molecules are immobilized below a critical off-pulse duration of about $T_{off}^c = 20$ ms, including the constant field (CF) case ($T_{off}^c = 0$) already shown in Figure 2a. When $T_{off} > 20$ ms, the molecules move, and for $T_{off} > 100$ ms the velocity reaches a plateau level. It is also noted that within the uncertainty of the measurements there is no difference between supercoiled and relaxed DNA in the unhooking behavior in intermittent fields (Figure 3b), as was the case in inverted fields.[13]

Electrophoretic Orientation in Constant Low or High Fields. Further insight into migration mechanisms was gained by studies of the electrophoretic orientation of the DNA molecules. The LD responses of one circular DNA and its two linear controls to pulses of constant electric field of two different strengths (3.8 and 22.5 V/cm) are compared in Figure 4, where the LD is expressed in terms of the orientation factor S according to eqs 1 and 2. Relaxed circular pIBI DNA ("Re") exhibits orientation parallel to the applied field ($S > 0$) at the high field strength, but unexpectedly the orientation is perpendicular ($S < 0$) at the low field strength. The linear form of pIBI ("Lin") is oriented parallel at both field strengths and so is a smaller linear fragment ("Lin/2") with approximately half the contour length of pIBI (for the shorter linear molecule only the response at 22.5 V/cm is shown).

The LD can be interpreted in terms of the orientation factor S (as is done in Figure 4) because of two observations. At either field strength no LD responses were observed at 300 nm, where DNA does not absorb light, nor at 260 nm in a DNA-free gel (not shown). This shows that the LD responses on which Figure 4 is based are not due to gel orientation[23] but indeed reflect DNA orientation effects. Secondly, the negative value of S at low fields (Figure 4) is derived from a positive LD, which in

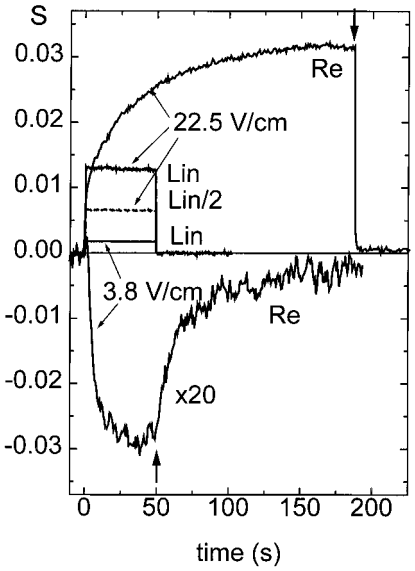

Figure 4. Constant-field LD response (260 nm) of nicked circular (Re) and linear (Lin) pIBI30 DNA (2926 base pairs) and linear 1353 base pairs DNA (Lin/2) in 5% polyacrylamide. Indicated field strengths were applied at time = 0 and turned off after 200 s (Re at 22.5 V/cm) or 50 s. The orientation factor was calculated as in eq 3.

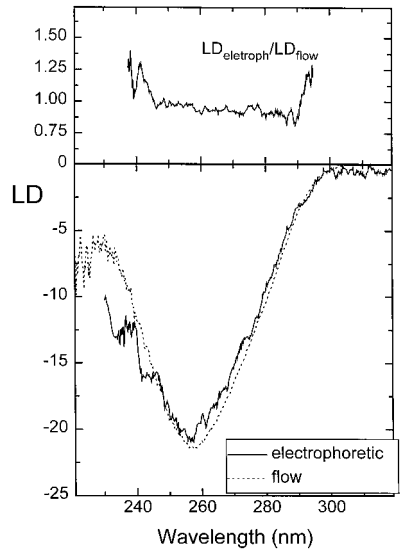

Figure 5. LD spectra of ΦX174 DNA during electrophoresis in polyacrylamide gel and of T2 DNA in a cuvette flow cell (from ref 24). The close similarity of the spectral shapes shown by the ratio being nearly independent of wavelength indicate that the DNA attains the same B-form under both conditions.

principle instead could have resulted from field-aligned DNA ($S > 0$) with a drastically changed secondary structure leading to a positive optical factor in eq 23 (such DNA forms have been observed in certain nonaqueous solvents[25]). The electrophoretic LD spectrum of DNA in polyacrylamide (Figure 5), however, has the same shape as that for flow-oriented DNA in electrophoresis buffer.[26] This observation supports that the DNA is close to its B-conformation during migration in polyacrylamide gels, as it is in agarose gels.[27] The LD time profiles thus reflect changes in helix orientation (S) and not in the DNA secondary structure (optical factor).

In addition to the opposite direction of orientation, the two modes of circle behavior at low and high fields differ markedly in terms of their orientation kinetics (Figure 4). Roughly speaking, the perpendicular mode is characterized by fast (seconds) build-up and slow (tens of seconds) relaxation. By

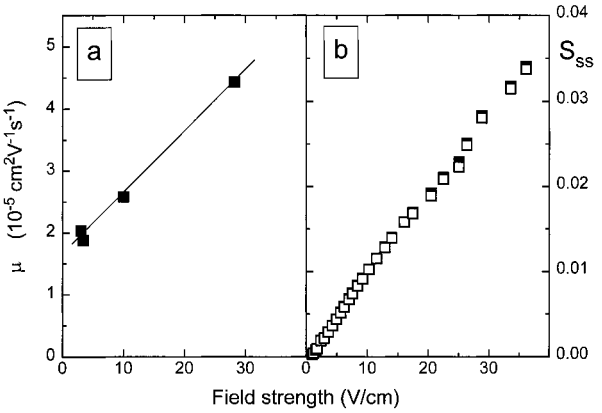

Figure 6. Constant-field electrophoretic orientation mobility (a) and orientation (b) of linear pIBI DNA vs field strength. Uncertainty in a indicated by the close overlap between two independent series (full and open symbols) and in b by the two independent measurements at 4 V/cm.

contrast, for the parallel component it is the relaxation which is fast (subsecond), whereas the build-up is very slow (tens to hundreds of seconds), although it will be shown below that the parallel build-up also contains a very fast (millisecond) component.

At the field strengths studied here no perpendicular orientation ($S < 0$) was observed for pIBI, ΦX174, or ColE1 nicked circular DNA in 1% agarose gel or in 2% hydroxyethylated agarose gels (not shown). The latter gel has an average pore size of 340 Å,[28] which is between the typical pore sizes in the more open and the tighter parts of the polyacrylamide gel.

Three Modes of Migration for DNA in Polyacrylamide Gels. The perpendicular orientation ($S < 0$) at low field strengths occurs only for the circles and not for either of the sizes of the linear form (Figure 4). This shows that the circle deviates from the behavior of linear molecules, be they either of the same contour length or of the same radius of gyration. The difference in orientation direction between circular and linear molecules is thus not an effect of differences in effective size but shows that the circles indeed have an inherently different mode of migration at low fields.

For the same reason (different direction of net orientation) the circles must migrate by different mechanisms at high and low fields. This is also in contrast to linear DNA, for which the direction of orientation is parallel at both high and low fields. On the basis of velocity and orientation data linear DNA was proposed to reptate in polyacrylamide gels at 22 V/cm.[13] Here we report that the electrophoretic mobility (velocity per unit field; Figure 6a) and the degree of electrophoretic orientation (Figure 6b) increase in a parallel manner with increasing field between 0 and 22 V/cm. In agarose gels such a concerted increase reflects migration by reptation.[4] Our working hypothesis will therefore be that in polyacrylamide gels linear DNA reptate in the whole range of field strengths investigated here. In total there are thus (at least) three modes of migration of DNA in polyacrylamide gels, one for linear and two for circular DNA

Transition from Perpendicular to Parallel Circle Orientation. Figure 7 reports how the orientation responses of the two circular forms change as the field is increased between the two strengths presented in Figure 4, i.e., during the transition from perpendicular to parallel net orientation. It is seen that the orientation kinetics (build-up and relaxation) at those intermediate fields is complex, and as discussed in detail below, this is because the parallel and perpendicular components occur

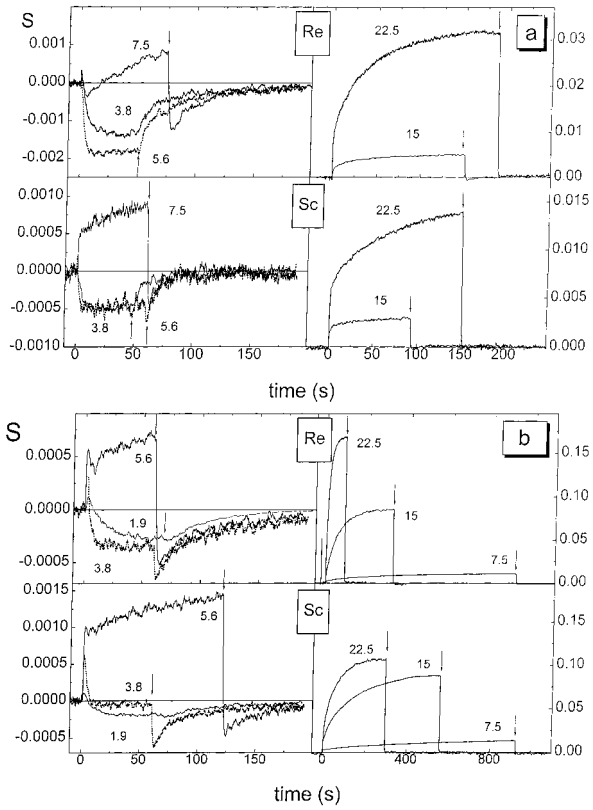

Figure 7. Constant-field LD response of supercoiled (Sc) and nicked (Re) pIBI DNA (a) and ΦX174 DNA (b) at indicated field strengths (V/cm). Field is applied at time = 0, and turned off at arrow.

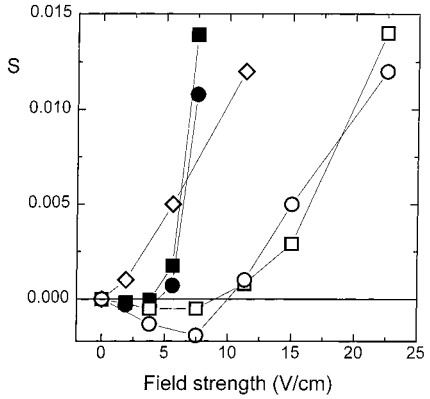

Figure 8. Steady-state orientation from Figure 7 vs field strength for pIBI (open) and ΦX174 DNA (full) of the supercoiled (squares), relaxed (circles), and linear (diamonds) form.

simultaneously and that they have very different orientation kinetics (Figure 4). Initially we focus on the steady-state orientation which is finally reached at each field strength. For nicked pIBI DNA (Figure 7a, upper panels) the steady-state orientation first decreases (becomes more negative) between 3.8 and 5.6 V/cm and then changes gradually from perpendicular to parallel. A similar transition occurs for supercoiled pIBI DNA (lower panels in Figure 7a) and for both circular forms of ΦX174 DNA (Figure 7b). The repeated pattern strengthens the notion that a circular topology is the crucial property for the two-mode behavior. Figure 8 summarizes how the degree of steady-state orientation of the different DNA forms depend on the field strength. Linear DNA is seen to exhibit a monotonous increase in S_{ss} with increasing field, whereas all four circle forms exhibit a (negative) minimum. It is also seen that the larger molecule (ΦX174) turns to parallel net orientation

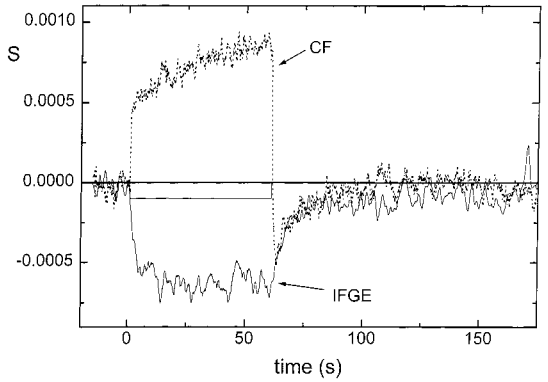

Figure 9. Constant (CF) and intermittent (IFGE: $T_{on} = 0.1$ s; $T_{off} = 1.1$ s) field response of supercoiled pIBI DNA at 7.5 V/cm.

at lower fields than does the smaller plasmid (pIBI), and that the two topological forms of the same size behave rather similarly.

For the investigation of the orientation kinetics it was desirable to find conditions under which the parallel and perpendicular orientation modes could be studied in their pure forms. Figure 8 shows that this can be accomplished by choosing a high or low field strength, respectively, as in Figure 4. At an intermediate field strength the two modes can be resolved by using pulsed fields to exploit their different kinetics (cf. Figure 4), as demonstrated in Figure 9 for relaxed pIBI DNA at 7.5 V/cm. Short (0.1 s) field pulses alternated by longer (1.1 s) field-free pauses (IFGE in Figure 9) favors perpendicular orientation (slow relaxation) over parallel orientation (slow build-up, fast relaxation). The result is a perpendicular orientation under conditions where a constant field (CF) gives a net parallel orientation. Interestingly, after the parallel (positive) component observed with the constant field has relaxed (in less than a second), there remains a perpendicular contribution which is seen to relax in the same slow manner as the perpendicular orientation which is produced in the IFGE case. The example of Figure 9 shows that in constant intermediate fields both orientation modes are present simultaneously and illustrates how pulsed fields can be used to resolve the two components.

Kinetics of Parallel Orientation. *Two Components of Build-up*. The kinetics of the parallel component ($S > 0$) is most easily studied at high fields because then the relative contribution from the perpendicular orientation is small, especially for the larger ΦX174 (Figure 8). The orientation grows faster for the relaxed than for the supercoiled form of ΦX174 (Figure 10a), but in both cases the build-up is dominated by a single-exponential component (Figure 10b, solid) which represents about 80% of the amplitude.[13] Analysis of this major parallel component has given a field dependence of the corresponding time constants which support an impalement mechanism.[13] Here we focus on the minor component which remains when the fitted main contribution (Figure 10b, solid) has been subtracted from the measured build-up response. The residual component ("Res" in Figure 10a) exhibits a fast rise, followed by a decay which at long times is monoexponential with a very similar time constant as the main component (Figure 10b, dotted). Measurements at higher time resolution (Figure 10a, inset) show that the fast rise part is approximately single-exponential with a rise time (t_f) of 15 ms.

Also with pIBI do both the nicked and supercoiled forms exhibit a dominating long-time single-exponential growth[13] preceeded by a minor transient component (not shown), which rises on the millisecond time scale and decays as the slow

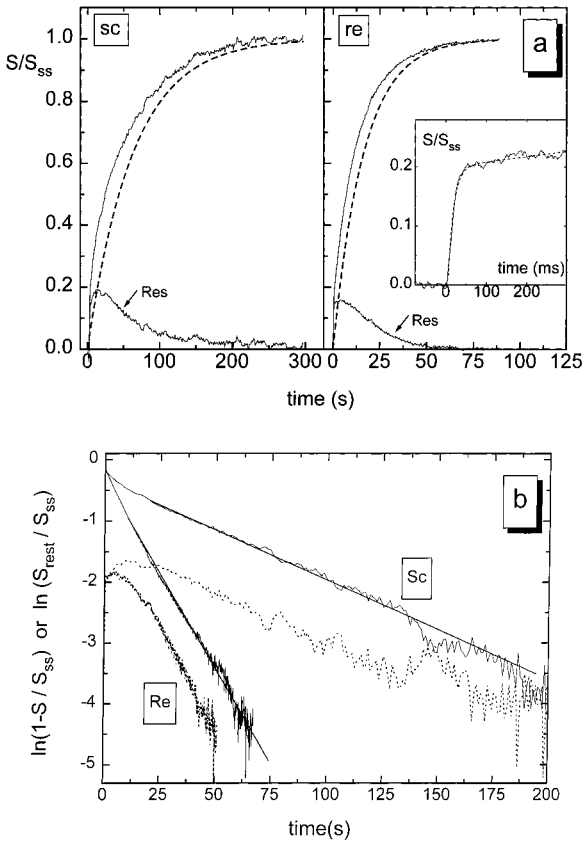

Figure 10. Build-up of orientation for supercoiled (sc) and nicked (re) ΦX174 DNA at 22.5 V/cm applied at time = 0: (a) Full curve, observed response; dotted curve, best fit to monoexponential growth at long times from panel b. Res, residual after subtraction of monoexponential part from observed response; inset, initial part of response for nicked form (full line) and fit (dotted line) to $S/S_{ss} = A(1 - e^{t/t_f}) + Bt$, with $t_f = 15$ ms; (b) semilogarithmic plot of observed response (full curve) and of residual (dotted curve) in panel a. Best linear fits at long times (lines) correspond to time constants 61 and 17 s for supercoiled and relaxed forms, respectively.

component grows in. It is concluded that this pattern is general for the parallel orientation mode of circular DNA.

Information from Inverted Fields. An important key to the understanding of the fast component of the parallel orientation came from experiments with symmetrically inverted fields (Figure 11). If the field is reversed periodically each 0.1 s, the observed orientation is constant as a function of time (Figure 11a). This level corresponds to the amplitude of the fast parallel component ($t_f = 15$ ms in Figure 10a, inset), as can be seen if the (still symmetric) pulses are extended to 5 s which gives a "sawtooth" response (Figure 11a): the slower parallel component sets in when the response has reached the level observed with 0.1 s pulsing. When the field is reversed after 5 s, the orientation rapidly drops to this level and then grows slowly again. The constant level is observed for symmetric pulse times between approximately 300 and 20 ms (regime II). Below 20 ms (regime I) the response is still constant in time, but the amplitude decreases as the pulses are made shorter. More precisely, by plotting the maximum and minimum amplitudes (which coincide in regimes I and II) vs pulse time (Figure 11b) it is seen that the sawtooth response sets in above 290 ms (regime III). This plot also gives the more exact value of 16.3 ms for the border between regimes I and II (Figure 11b, inset).

Field-Free Orientation−Relaxation of the Parallel Component. The relaxation of the parallel component was studied as a function of the length (T_p) of the orienting field pulse at 22.5

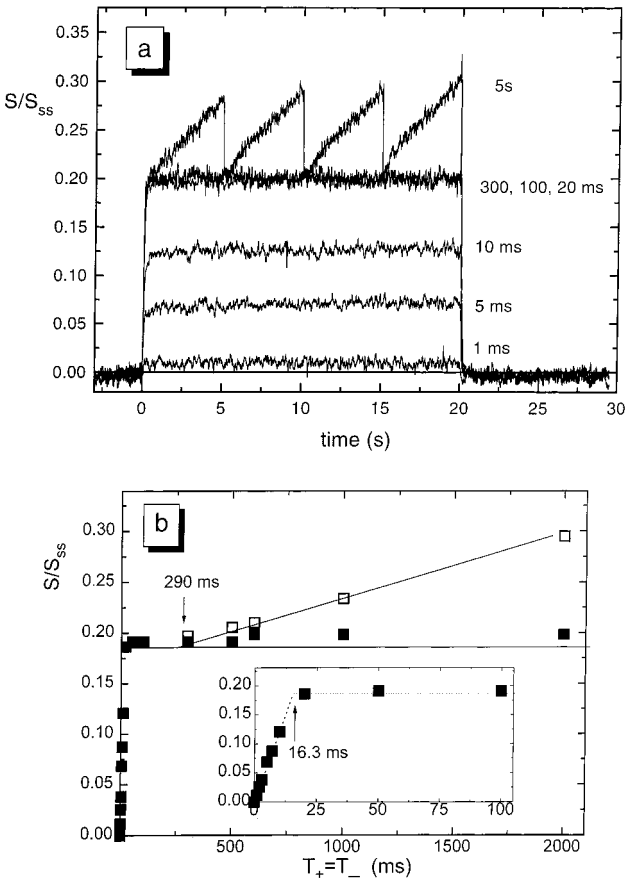

Figure 11. Electrophoretic orientation of supercoiled ΦX174 DNA in field inversion gel electrophoresis with symmetric pulses ($T_+ = T_-$) at 22.5 V/cm: (a) Time responses at indicated pulse durations; (b) maximum (open symbols) and minimum (full symbols) orientation during a pulse cycle vs pulse duration.

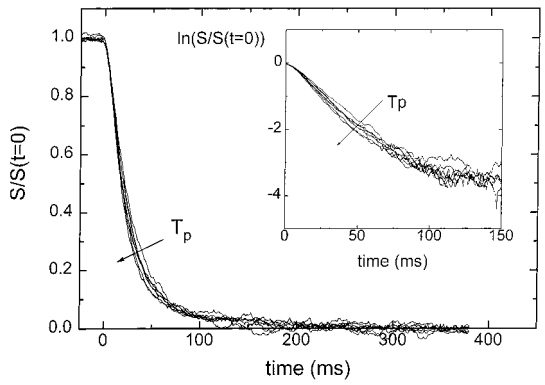

Figure 12. Field-free orientation relaxation of supercoiled ΦX174 DNA at 22.5 V/cm (turned off at time zero) vs duration T_p of the orientating pulse (i.e., field was turned on at $-T_p$). Arrow indicates responses in order of increasing T_p = 1, 5, 10, 20, 69, 120, and 240 s. The responses have been normalized to the *S*-value at the time of field removal. Inset: Semilogarithimic plot.

V/cm, i.e., at different positions along the slow build-up in Figure 10a. In Figure 12 the responses have been normalized to the *S*-value, which had been reached when the field was turned off T_p seconds after its application. It is seen that the decay profiles are very similar, with only a weak trend toward faster relaxation the further the build-up has proceeded. The relaxation is not monoexponential (inset), but throughout the orientation build-up the decay could be fitted satisfactorily by two exponentials. The slower one, with a time constant of 120 ± 30 ms, was responsible for less than 5% of the decay

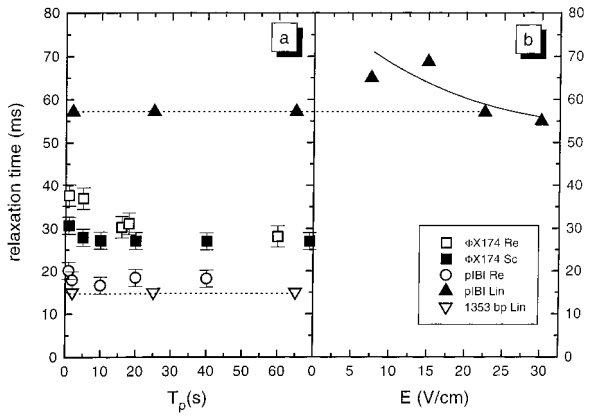

Figure 13. Decay time constants for the major parallel orientation component of the field-free relaxation as in Figure 12 for the supercoiled (Sc), nicked (Re), and linear (Lin) forms of the indicated DNA sizes: (a) time constants vs pulse duration at 22.5 V/cm; (b) time constant for linear pIBI (which is independent of T_p) vs field strength.

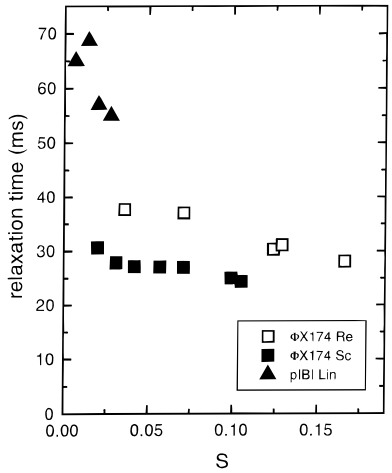

Figure 14. Decay time constants from Figure 13 plotted vs degree of orientation at the time of field removal.

amplitude. The main faster component had a time constant of about 25 ms for the supercoiled ΦX174. The nicked forms of both PIBI and ΦX174 also exhibited almost monoexponential decays for the parallel component (not shown). Figure 13a summarizes the corresponding (fast) relaxation times $\tau_{||}$ for the main component at different stages of the build-up and compares them with the corresponding relaxation times of linear DNA of two sizes, pIBI and the 1353 base pair fragment. For linear DNA the relaxation rates are seen to be independent of pulse duration, as expected since there is no change in orientation (Figure 4). For the circles there is initially a slight decrease in the relaxation time with increasing pulse duration (as seen already in the raw data, Figure 12), but the ΦX174-circle relaxation times are always shorter than for the corresponding linear molecules of (approximately) half the size ("pIBI Lin"). By contrast the nicked circles of pIBI relax more slowly than their linear halves but faster than the full-sized linear counterpart. There is no significant difference between supercoiled and relaxed circles in the relaxation of the parallel orientation.

For linear pIBI the relaxation time decreases slightly with increasing field strength (Figure 13b), i.e., with increasing degree of orientation. This observation give rise to the possibility that the ΦX174 circles relax more rapidly than their linear controls because of the higher degree of orientation of the circles (Figure 4). In Figure 14 the relaxation times for circles and linear molecules are therefore compared on the basis of the degree of

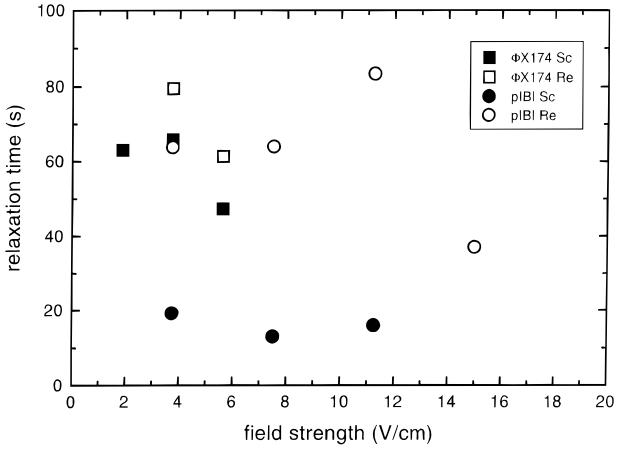

Figure 15. Time constants vs field strength for the field-free relaxation of the perpendicular orientation component for the supercoiled (Sc) and nicked (Re) forms of the indicated DNA sizes.

orientation. It is seen that linear pIBI has a longer relaxation time also in the narrow region where the *S*-values overlap, which shows that the circles relax faster for a reason other than their higher degree of orientation.

Kinetics of the Perpendicular Orientation. *Field-Free Relaxation*. The perpendicular orientation ($S < 0$) relaxes monoexponentially (not shown), with a time constant $\tau_\perp$ (Figure 15), which is essentially field-independent in view of the strong scattering of the data. It is also seen that the supercoiled PIBI relaxes faster than do the nicked PIBI and both forms of ΦX174. A more important observation is that the time constant $\tau_\perp$ for the circles is of the order of tens of seconds. This is much longer than the relaxation time of approximately 70 ms for the linear form at the same low fields (Figure 13b), which shows that under the present conditions the Brownian dynamics of circular DNA in gels can be much slower than for linear DNA of the same size. The high values for $\tau_\perp$ also means that the perpendicular orientation relaxes much more slowly than the parallel component ($\tau_{||}$ in Figure 13a). This indicates that the environment in which the two types of circle orientation occur are very different.

Build-up of Perpendicular Component. The build-up of the perpendicular component ($S < 0$) is most easily studied for the smaller pIBI, since the competing parallel orientation becomes significant first at considerably higher fields compared to the larger and therefore more easily impaled ΦX174 (Figure 8). For the relaxed pIBI circle (top row in Figure 7a) the time to reach the steady state (t_{ss}) is 25 s at 3.8 V/cm and 10 s at 5.6 V/cm, a decrease which is expected due to the stronger orienting electric force.[4] The supercoiled form also exhibits rates of perpendicular build-up which increase with increasing (but still low) fields (3.8 and 5.6 V/cm in the bottom row of Figure 7a).

The two topological forms differ, however, in the degree of orientation. At any of the two fields the magnitude of the (negative) *S* is lower for the supercoiled form, and one contributing factor is that the supercoiling turns will reduce the degree of orientation of the helix axis with respect to the field by about 40% for the present degrees of supercoiling.[13] This tertiary-structure effect cannot change the sign of the LD response,[13] however, and can therefore not explain the presence of both negative and positive values of *S* during the responses at intermediate field strengths, such as the next higher field strength of 7.5 V/cm in (Figure 7a). The explanation instead has to be found in the dynamic mixing of perpendicular and parallel orientations revealed in Figure 9 and how this phenomenon is affected by circle topology.

Orientation Behavior at Intermediate Fields. *Supercoiled DNA and Its Smaller Tendency To Orient Perpendicularly*. Figure 8 shows that DNA size is the most important factor for determining at which field strength the net orientation turns positive. Topology also plays a role, however, as can be seen by a careful analysis of the responses in Figure 7. With pIBI (Figure 7a) the relaxed form is more perpendicularly oriented (*S* is more negative) at 5.6 than at 3.8 V/cm, whereas the *S*-amplitude for the supercoiled form is the same at the two field strengths. This indicates an opposing positive contribution which is larger for the supercoiled form, and this trend is continued at 7.5 V/cm, where both forms have a positive steady-state orientation but the supercoiled form more so. An important clue to the understanding of the effect of circle topology can be found in the field-free relaxation behavior at this field strength. The parallel component relaxes in about 30 ms (Figure 13a) and results in a negative *S*-value corresponding to the long-lived perpendicular component, which relaxes back to $S = 0$ over a period of tens of seconds. The relative contributions to the net orientation at the time of field removal can be estimated by comparing the relative amplitudes of the fast positive and slow negative relaxation amplitudes. At 7.5 V/cm the ratio is about 3 for the supercoil and 2 for the nicked form, showing that the parallel contribution is more dominant for the supercoiled form at a this field strength. A similar analysis shows that at 3.8 V/cm the orientation indeed is purely perpendicular for both circle forms since they lack the fast relaxation component. At 5.6 V/cm the orientation is still purely perpendicular for the relaxed form, but a small positive relaxation component for the supercoiled form reveals a weak parallel component. This explains why the steady-state orientation amplitude for the supercoil does not increase even though the electric force is increased by increasing the field from 3.8 to 5.6 V/cm: the expected increase in perpendicular orientation is offset by the emergence of a parallel contribution.

This approach of exploiting the relaxation amplitudes is very fruitful for sorting out the complex orientation behavior at intermediate fields. The analysis confirms that the minimum in Figure 8 occurs as a result of a competition between the perpendicular orientation, which exists in pure form at low enough fields (Figure 4), and the perpendicular orientation which grows in as the field is increased and molecules become impaled. The comparison of the two circle topoisomers shows that the parallel component becomes dominant at lower fields for the supercoiled form. This is surprising since the relaxed form is more efficiently impaled,[13] and this observation therefore suggest that the process which leads to perpendicular orientation is less efficient for the supercoil.

For the larger ΦX174 (Figure 7b) the parallel component is relatively stronger (Figure 8), to the extent that a pure perpendicular orientation response is not observed even at the lowest field (1.9 V/cm in Figure 7b). There is an initial spike of fast parallel ($S > 0$) orientation (cf. Figure 10a, inset), and from this rapidly established positive level the perpendicular orientation ($S < 0$) grows in. At 1.9 V/cm t_{ss} is about 50 s for both supercoiled and nicked circle, and it decreases to about 20 s as the field is increased to 3.8 V/cm. This increase in rate with increasing field is expected for the same reason as with pIBI, as is the higher value of t_{ss} for ΦX174 at a given field strength due to its larger size.

Also with ΦX174 does the supercoiled form exhibit a stronger tendency to turn to parallel orientation. At 3.8 V/cm the relaxed form has a steady-state value of *S* which is more negative than at 1.9 V/cm (Figure 7b, top row), whereas the supercoiled form

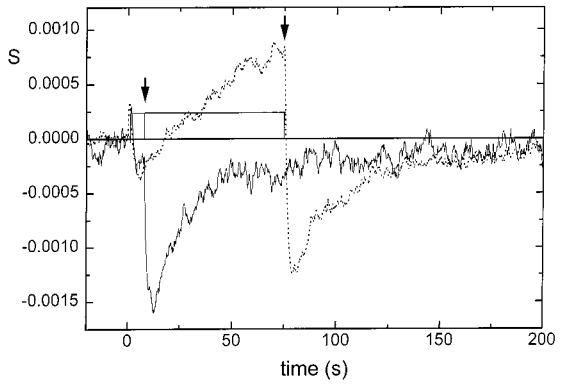

Figure 16. Constant field response of nicked pIBI DNA at 7.5 V/cm to field pulses of 5 (solid lines) and 75 s (dotted lines) duration. Field profile indicated.

has a net *S* which is less negative at 3.8 V/cm and in fact close to zero (Figure 7b, bottom row). The relaxation amplitudes reveal that the latter effect again is due to a cancellation between significant negative and positive contributions, this time of nearly identical amplitudes.

Simultaneous Existence of Parallel and Perpendicular Orientations throughout the Build-up. The above analysis also shows that the two orientation components occur side by side in the steady state. The relative contribution of the two modes during the build-up to the steady state can be studied by performing a field-free relaxation analysis after pulses of different duration. Using the relaxed pIBI at 7.5 V/cm as an example, this can be used to show that the positive component is present at all times, even if the net orientation is perpendicular initially (Figure 16). At the end of a short 5 s pulse (left arrow above square-shaped field profile) *S* is negative, but the relaxation amplitudes show that this level is the net result of the negative component being partly cancelled by a positive contribution of comparable but lower magnitude. After the longer pulse (75 s, right arrow) *S* has become positive because the slow positive component has grown and now contributes about two times as much as the perpendicular component. The presence of a positive relaxation early in the response shows that there is a very fast (subsecond) parallel component also at low fields (just as in strong fields, inset of Figure 10a), which again can be seen to give rise to a small positive spike in Figure 16 just after the field is applied.

Figure 17 shows a more extensive analysis of relaxed ΦX174 DNA at 7.5 V/cm (see Figure 7b for the steady-state response). The absence of a negative relaxation component for a short pulse (0.2 s in Figure 17a) shows that initially there is only a purely positive component, which has a rise time of about 100 ms. This value is consistent with the shorter rise time $t_f = 15$ ms observed at the higher field of 22.5 V/cm (Figure 10a, inset). However, in contrast to the continued growth (albeit slower) at 22.5 V/cm, at 7.5 V/cm there is a slight tendency for *S* to decrease after the fast rise. This is more evident with the longer pulse used in Figure 17b, where a clear maximum in *S* is observed after about 0.1. This is the result of the apperance of the negative component which grows slowly (seconds, left panels in Figure 7b) compared to the millisecond kinetics of the fast parallel component. Still, it is fast compared to the slow parallel component which stems from impalement, which occurs over tens or hundreds of seconds (Figure 10). Since impalement is an efficient mechanism in orienting DNA, its final dominance results in the LD response in Figure 17b going through a minimum after about 1 s. After 10 s the ratio of the parallel and perpendicular components is about 5:1, as estimated from the relaxation amplitudes.

In Figure 17b the response is shown at two different sampling rates. The slower sampling rate is used in Figure 17c, which shows the long-time build-up of the parallel component, without the maximum and minimum due to the limited time resolution. Analysis of the relaxation amplitudes in Figure 17c shows that throughout the build-up the perpendicular component has an essentially constant amplitude and relaxation time $\tau_\perp$ (of approximately 60 s, cf. Figure 15) all the way to the steady state Figure 17d.

In summary, at all fields there are three modes of circle orientation: a fast parallel component, a slower perpendicular contribution, and finally a very slow parallel component. The last one is caused by impalement,[11] but the mechanisms behind the other two remain to be discussed.

Circle Orientation in Pulsed Fields. Figure 18a shows the LD time responses of supercoiled ΦX174 to intermittent fields, and how they depend on the duration of the field-free pulse (T_{off}), with a fixed $T_{on} = 1$ s. (The corresponding velocity data are in Figure 3b). For T_{off} values of less than 6 ms the response is indistinguishable from the CF response, with its fast initial component and subsequent slow growth (cf. Figure 7b). For longer field-free pulses the magnitude of the initial component fast part is retained, but the slow component decreases in amplitude and acquires an oscillatory behavior. For T_{off} above approximately 50 ms the orientation starts to drop below the level of the fast component at the lowest point in each off-pulse, and above approximately 200 ms the orientation relaxes almost completely in each cycle. A plot of the *S*-amplitude (at 20 s and normalized to the CF value) vs T_{off} (squares in Figure 18b) gives a more precise value of the critical field-free pulse of $T_{off}^c = 5.9$ ms (Figure 18b, inset), below which the response is indistinguishable from the CF response. This is the necessary diffusion time for unhooking, since the CF response is expected if molecules are not unhooked during each pulse cycle.

In order to check the consistency of the pulsed-field approach of Figure 18, the corresponding data were collected for $T_{on} =$ 20 ms instead of 1 s (circles in Figure 18b). A forward pulse of 20 ms is too short to impale the molecules,[13] and the curve should therefore reflect the field-free decay of the fast parallel component. The decay time constant for S/S_{cf} is seen to be approximately 30 ms, in agreement with Figure 13a.

Discussion

The present study shows that circles and linear molecules migrate by very different mechanisms in polyacrylamide gels, as reflected in both orientation and velocity. The strikingly complex, behavior can only be understood if the heterogeneous structure of this gel is taken into account. It is therefore important to note that the gels were prepared at a temperature which is low enough to promote a heterogeneous gel structure.[29]

Migration at High Fields. *Further Support for Impalement.* In the earlier study it was proposed that at high-field circles are impaled on gel fibers, whereas linear molecules migrate by reptation.[13] Here reptation by the linear form is further supported by the results of Figure 6. The impalement mechanism for the circles is supported by pIBI DNA requiring a stronger field than ΦX174 in order to become oriented parallel to the field (Figure 8), since the smaller molecule will experience less electric force to keep it impaled. This point has been made earlier by Mickel et al.[10] on the basis of velocity measurements in agarose. The absence of topology effects in the detrapping by intermittent (Figure 3b) or reversed[13] fields, in spite of the

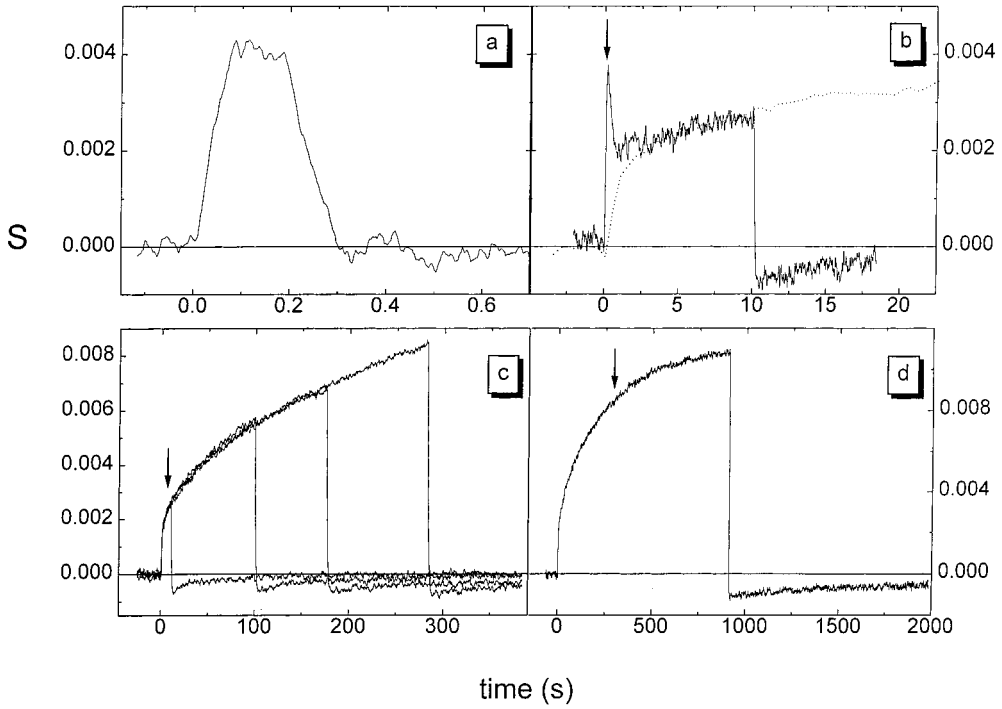

Figure 17. Constant field response of nicked ΦX174 DNA at 7.5 V/cm to field pulses of durations 0.2 s (a), 10 s (b), 10, 100, 170, and 190 s (c), and 850 s (d). Arrows indicate position of field removal in previous panel. Sampling times: (a) 0.5 ms; (b) 10 ms and 64 ms (dotted line); (c) 64 ms; (d) 64 ms.

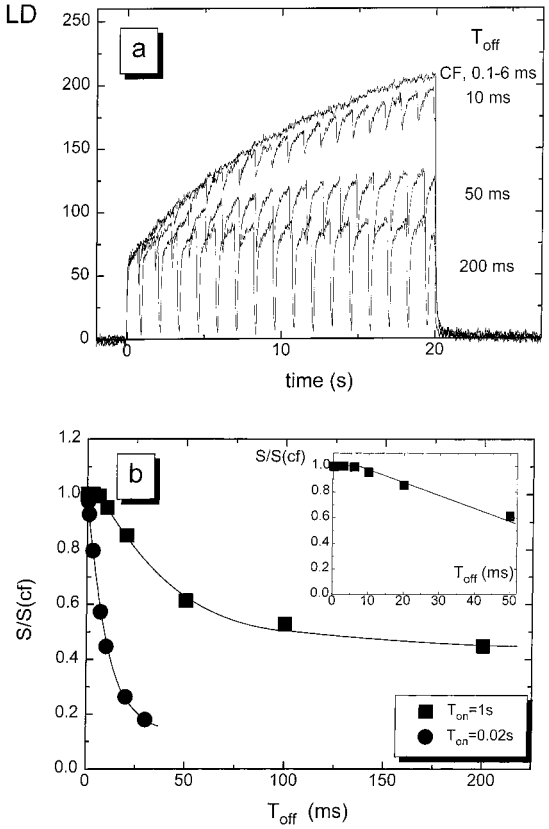

Figure 18. Electrophoretic orientation of supercoiled ΦX174 DNA in intermittent field gel electrophoresis at 22.5 V/cm: (a) time responses with $T_{on} = 1$ s at indicated durations T_{off} of the field-free pause; (b) maximum orientation amplitude (normalized to constant field amplitude) vs T_{off} for indicated values of T_{on}.

trapping kinetics being topology sensitive (Figure 7), is also consistent with impalement. The effective hole size should be important for the probability (and therefore rate) of impalement but has much less effect on the rate with which the molecule can be pulled off from the fiber once it is caught.

Impalement Preceeded by Migrative Orientation. In the total LD response, immobilization by impalement is responsible for the slow major component in the parallel orientation (Figure 10a), but it cannot explain the fast-rising ($t_f = 15$ ms) minor residual component ("Res" in Figure 10a) since a permanent trapping cannot explain a transient response. In fact, the observation that the residual component decays with about the same time constant as the impalement component grows (Figure 10b) indicates that the two underlying processes are coupled in a reciprocal manner, as expected if the transient component represents an orientation contribution from the subpopulation of molecules which are yet to become impaled.

Importantly, for (symmetric) pulse times between about 20 and 300 ms the whole population of molecules attain the orientation level of the residual component (Figure 11a). Earlier results show that in this pulse range the circular molecules migrate with a velocity characteristic of nonimpaled molecules: the forward pulse is short enough to avoid appreciable impalement and the backward pulses long enough to unhook those molecules which still have become impaled. These velocity data thus strongly indicate that the constant level observed for pulsing at intermediate frequencies ($0.2S_{ss}$ in Figure 11a) result when the molecules migrate back and forth without any appreciable impalement.

In fact, under this interpretation the collected velocity[13] and orientation-kinetics data in strong fields (Figures 10a and 13a) can explain the existence of three regimes of orientation behavior in symmetric pulsing (Figure 11b). In regime I ($T_+ = T_- < 16$ ms) pulse times are shorter than the rise time $t_f = 15$ ms (Figure 10a, inset), and the amplitude is therefore lower than that for full migrative orientation. In regime II the pulses are long enough to orient the molecules migratively, and the orientation remains at this level until the pulses are long enough to lead to onset of impalement. According to less precise

velocity data[13] this occurs with a forward pulse of 0.6 ± 0.3 s, in fair agreement with the value of 0.29 s obtained for the end of regime II. In both I and II the degree of orientation is constant in time because for migrative orientation at 22.5 V/cm the relaxation time (30 ms, Figure 13a) is longer than the rise time (15 ms), so the molecules remain oriented as they are shuffled back and forth. In regime III the effect of impalement (in each pulse direction) is reflected by *S* raising above the migrative level to the same extent in both directions (since the pulses are equally long in both directions), as exemplified by the 5 s pulses in Figure 11a. The orientation drops to the migrative level after each field reversal because the relaxation time for impalement orientation (30 ms) is much shorter than the rise time of tens or hundreds of seconds.

In conclusion the collected data strongly support that the fast component of the parallel orientation (with an amplitude of $0.2S_{ss}$ in Figure 10a) is caused by migration. Its rise time of $t_f = 15$ ms is consistent with a migrative type of orientation, since a similar value (25 ms at 22.5 V/cm) is observed for the rise time of the linear form of the same length,[13] which is known to orient by migration. Thus, the drop in *S* down to the level of migrative orientation during each field reversal (5 s pulses in Figure 11a) reflects in an illuminating way how the molecules unhook from one set of impalements and for about 0.3−0.5 s are oriented only by migration as they are on their way to being impaled on a new set of fibers in the opposite direction.

Two-State Model for the Parallel Mode. The fast migrative orientation is followed by the slow growth of *S*. This process is too slow to reflect a conformation change in individual molecules, a conclusion which is also supported by the strong field dependence in the growth rate.[13] We instead propose that the slow growth reflects the transfer of molecules from the pool of migrating molecules (low *S*) to the ensemble of impaled molecules (high *S*). The slow rate of growth reflects how long it takes to find a trap, rather than the time it takes to attain the more field-aligned conformation once the molecule is impaled. (The latter process most likely occurs on the millisecond time scale because it only involves the motion of different parts of the molecule relative to each other.)

The two-state model of the circle behavior at high fields was tested by comparing the constant-field LD response with the function

$$S(t)/S_{ss} = A(1 - e^{-t/\tau_f})e^{-t/\tau_{imp}} + (1 - e^{-t/\tau_{imp}}) \qquad (3)$$

where S_{ss} is the steady-state level of orientation, $A = 0.2$ is the amplitude (relative to S_{ss}) of the constant level at intermediate pulse times in Figure 11a, $t_f = 15$ ms (Figure 10a), and τ_{imp} is determined from the long-time slope of the full response (Figure 10b). The first term in (3) corresponds to the creation of an ensemble of migratively oriented molecules (τ_f) and how it decays exponentially with the characteristic impalement time (τ_{imp}) as the molecules become trapped. The second term reflects the increasing concentration of impaled molecules. Figure 19 shows that eq 3 describes the main characteristics of the observed response except for a small transient residual which indicates that a complete description of the development of the migrating ensemble requires a second intermediate with a rise time of about $\tau_{imp}/5$.

The fact that the field-free relaxation of the parallel component occurs with essentially the same time constant throughout the build-up (Figure 13a) shows that the trapped molecules are in very similar states whether caught early or late in the process, which explains the relative success of the two-state model of eq 34. The slight initial decrease in the average relaxation time

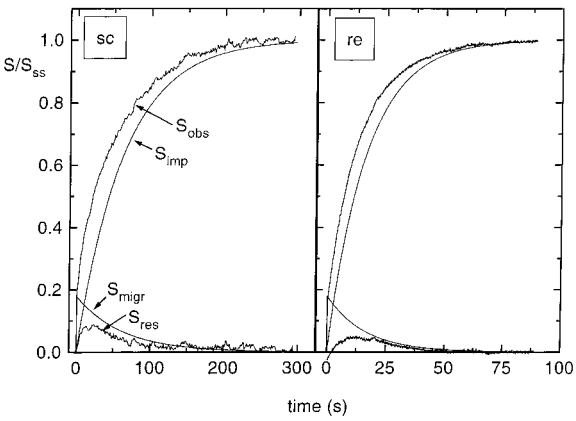

Figure 19. Resynthesis of the observed (obs) build-up of orientation for supercoiled (sc) and nicked (re) ΦX174 DNA at 22.5 V/cm (see Figure 10), according to eq 3, in which the first and second terms correspond to curves "migr" and "imp", respectively. The residual (res) is obtained by subtracting the sum of imp and migr curves from the observed response.

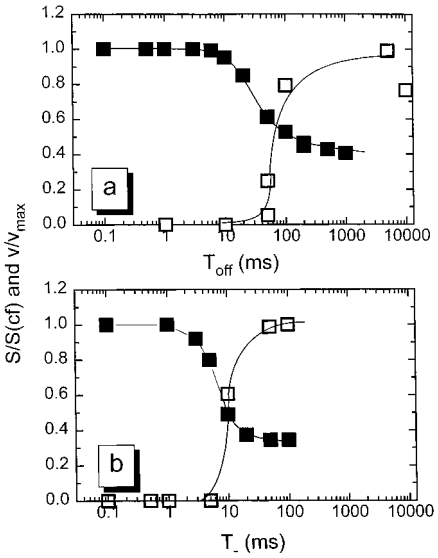

Figure 20. Normalized orientation (*S*; solid) and velocity (v; open) vs (a) duration of field-free pause (T_{off}) in intermittent field electrophoresis and vs (b) duration of reversed field (T_-) in inverted field electrophoresis. Data in a from Figures 3b and 18. Data in b from ref 13.

(Figure 13a) shows that free-migrating molecules relax somewhat more slowly, probably because they are under less tension than the impaled molecules.

Detrapping. *Use of LD To Study Detrapping*. If the amplitude of the LD signals in intermittent fields in Figure 18 (taken as the peak value at 20 s) is plotted vs T_{off} (Figure 20a), there is a correlation with the corresponding velocity data (from Figure 3b). The drop in orientation occurs essentially in parallel with the onset, growth, and approximate saturation of the electrophoretic velocity. This is consistent with the major LD component being from impaled molecules, since as the molecules are detrapped, they also lose orientation. A similar correlation between orientation and velocity was found when the molecules were detrapped by inverted fields[13] (Figure 20b). It is seen that the midpoint of detrapping occurs for shorter pulses in inverted rather than in intermittent fields, which is expected since it should be faster to pull the molecules off the fibers than letting them diffuse off passively.

Use of LD and Velocity To Measure Different Averages of the Detrapping Time. Interestingly, the velocity and LD

curves in Figure 20 are not symmetric around the crossing point, since the LD curves start to drop before the velocity curves start to increase. Therefore, in intermittent fields the LD-derived critical detrapping time (6 ms from the inset of Figure 18b) is shorter than the value of obtained from velocity (about 50 ms, Figure 20a). Similarly, in inverted fields (Figure 20b) the backward pulse duration required for detrapping is 1.3 ms according to LD[13] and therefore shorter than the 5 ms obtained with velocity.[13] It is proposed here that this difference reflects that LD and velocity probe the distribution of trap depths differently.

In the velocity approach detrapping is defined by the actual velocity of the zone being nonzero; i.e., the backward/off pulse is long enough to detrap the molecules from all traps. By contrast, in LD the critical pulse time is defined by the deviation from the constant field response, which occurs when the first molecules are detrapped. Since these molecules are the ones in the most shallow traps, this takes shorter pulses than complete detrapping. These shorter pulse durations do not release the molecules definitely but only force them to (on the average) migrate somewhat further until they find traps which are too deep to allow detrapping at that particular backward/off pulse duration. This explains why for a certain range of intermediate pulse durations in Figure 18a the slow component is still present (because sooner or later the molecules become trapped) but with a slower rate of growth (because the trapping is less efficient since there are fewer effective traps).[13] Consistent with this interpretation, actual zone movement (i.e., a nonzero zone velocity in Figure 20a,b) do not occur until (approximately) the corresponding LD curves have reached the lower plateau level at longer pulses, which above has been ascribed to migrative orientation.

Calculation of Translational Diffusion Coefficient from the Detrapping Times. Irrespective of the comparison being based on LD or velocity data, the pulse duration for detrapping is 4−6 times longer in intermittent fields than in inverted fields (Figure 20a,b). These data can be combined to calculate an effective translational diffusion constant in the gel. The average length L_f of the impalement fiber was calculated[13] from the critical backward detrapping time to be 8.7 and 33 nm, respectively, on the basis of LD or velocity. Using these values together with the critical off-times T_{off}^c for unhooking by field-free diffusion (as obtained with the same experimental technique), the diffusion coefficient can be calculated as $L_f^2/2T_{off}^c$ to be 2.7×10^{-10} cm^2 s^{-1} from velocity and 6.3×10^{-11} cm^2 s^{-1} according to LD data. These values are lower than the free solution value of 3.22×10^{-8} cm^2 s^{-1} for (supercoiled) circular ΦX174 DNA[30] by a factor of about 100, which again points to the strong effect of the matrix on the Brownian motion of these comparatively large DNA molecules.

Migration Modes at Low Fields. *Third Mode of Migration.* At low fields the circles cannot be migrating by the reptation mechanism of the linear form, since the perpendicular orientation observed at low fields (Figure 4) is inconsistent with transient anchoring and stretching. The same argument can be invoked against the migration/impalement mechanism which is operating for the circles at high fields. A third mode of migration and orientation for DNA is thus required in order to explain the circle behavior at low fields. The negative *S*-values observed at low fields (Figures 4 and 7) correspond to very low degrees of net orientation. This is partly due to cancelling effects between the concomitant parallel and perpendicular orientations, but the molecules must still be considered to be close to their equilibrium conformation. This means that a very wide distribution of conformations will be consistent with the observed net orientation, and molecular interpretations are correspondingly more difficult to prove than in the high-field case.

The impalement mode can occur at the same time as the unknown third mode, as seen from the presence of both orientation components at intermediate fields (Figures 7, 16, and 17). In principle, both components of the orientation could be present in each molecule at the same time, for instance if the molecules attain an L-shaped conformation, but this seems unlikely since it is hard to imagine that two orientation relaxation processes with a 1000-fold difference in rate can occur in the same molecule. The difference in relaxation rates rather indicates that the two types of orientation occur in different parts of the gel (see below). We therefore favor the picture that at any instant there are two populations, containing molecules which have opposite direction of net orientation and which reside in different parts of the heterogeneous gel structure. The LD contributions from the two populations can be resolved through the relaxation amplitudes (as in Figure 16), but they cannot be translated into molecular concentrations because the orientation per molecule in the two modes are not known.

Properties of the Perpendicular Mode. The most important clue to the mechanism behind the counterintuitive perpendicular orientation is its extremely slow relaxation. The perpendicular component needs tens of seconds to relax (Figure 15), whereas the parallel component relaxes in about 20−40 ms for the circles and 55−65 ms for the linear form (Figure 13). What is the source of the very slow decay of the perpendicular relaxation?

The rotational relaxation time for a 2900 base pairs molecule in free solution is about 0.9 ms for the linear form[31] and 0.33 ms for the (supercoiled) circular form.[32] Thus all three orientation modes in the gel relax more slowly than in free solution, as expected since the gel matrix should slow down DNA rotation. The extent of the slowing down can in fact be expected to reflect the space available for the relaxation. Using transient electrical birefringence, Stellwagen[31] has shown that in agarose there is a 2-fold increase in the relaxation time for the 2900 base pairs (linear) DNA molecule (compared to free solution) when the average pore diameter is equal to the radius-of-gyration. It should be noted, however, that atomic force microscopy has later been used[33] to show that the average pore size is about 4 times larger than the values used by Stellwagen. The matrix can thus be expected to reduce the rotational rate more than 2-fold when the radius-of-gyration really is comparable to the pore size (such high gel concentrations were not included in the Stellwagen study).

For the linear pIBI we indeed find a considerably stronger effect, a 25-fold increase in the rotational relaxation time. This is consistent with the 10-fold increase (to 30 μs) for a smaller 207 base pairs linear fragment in a polyacrylamide gel (4% T, 10% T)[34] (larger molecules were not studied). For the circles we observe a similar 25-fold increase in the relaxation time for the parallel component (Figure 13), but for the perpendicular component the polyacrylamide matrix increases the relaxation time more than a 1000-fold (Figure 15) compared to solution. For the molecules studied here, the radii-of-gyration are comparable to the diameters of the largest cavities in the polyacrylamide gel. The important conclusion, in the spirit of Stellwagen,[31] is therefore that the relaxation rates of the impaled molecules are consistent with the relaxation occurring in the open parts of the gel, whereas molecules which are perpendicularly oriented must be confined in much tighter spaces in the gel than are the impaled molecules.

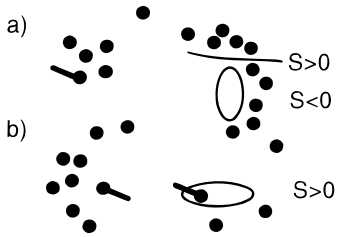

Figure 21. Suggested lobster (a) and impalement (b) traps for circular DNA in polyacrylamide gels.

Another important clue is that the net orientation turns parallel at lower field strengths with the supercoiled species (Figure 7), in spite of the nicked form being more efficiently impaled.[13] This suggests that the probability or capability of the supercoiled species to attain a perpendicular orientation is less than for the relaxed circle. Finally, we have not been able to observe the phenomenon of perpendicular orientation in agarose gels, not even in hydroxyethylated gels which have resolution capabilities (i.e., effective pore sizes) similar to those of polyacrylamide gels.

Possible Mechanism for the Perpendicular Orientation. One model that could account for these observations can be based on the observation that a circular molecule most likely cannot enter the dense parts of the polyacrylamide gel, but that a linear molecule can. The average pore size in these regions is as small as 60−90 Å,[18] which is larger than the helix diameter (20 Å) of DNA, but considerably smaller than its persistence length $P = 500$ Å. Since P is equal to the thermal-averaged radius-of-curvature of a DNA chain, there will be a substantial barrier in these pores against the loop formation a circle cannot avoid. Circles could then be trapped between dense regions if they happen to form narrow-ended channels ("lobster traps", Figure 21), whereas the linear form could reptate through the bottom of these traps. In this model the perpendicular helix orientation for circular DNA ($S < 0$) at low fields (Figure 4) can be explained by the field pressing the molecules up against the downfield wall of the traps, whereas linear DNA would be field-aligned ($S > 0$) as they reptate through the escape route (Figure 21). The propensity of the supercoiled molecules to enter these traps could be lower if the supercoiling led to larger global stiffness compared to the nicked circle. The less hindered perpendicular relaxation of the supercoiled form (at least for pIBI, Figure 15) may be an indication of this. An interesting observation in this context is that a compactation of circular DNA observed during electrophoresis in polyacrylamide gels has been suggested to occur more easily for the relaxed circle than for the supercoiled form.[35] Finally, such lobster traps may be more unlikely to exist in agarose gels, because there is no evidence for dense regions with pore sizes much smaller than the persistence length. In hydroxyethylated agarose the small pores do slow down loop formation[7] (with effects on the migration of linear DNA[28]) but does not prevent it.

Such lobster traps would give rise to the zone-broadening at low fields (Figure 2) if there is a broad distribution of trap depths, as can be expected from the heterogeneous character of the gel.[19] The presence of a negative component with an essentially constant amplitude throughout the trapping process (Figure 17c,d) suggests that there is always a population of perpendicularly oriented molecules which is not free to join the ensemble of impaled molecules. In this sense they are trapped, which adds credibility to the concept of a lobster-trap mechanism for perpendicular orientation. It should be remembered, however, that impalement may contribute to the slow migration and wide zones at low fields, because below about 15 V/cm the field is not strong enough to keep the circles permanently impaled.[13]

Brownian Motion of Circular DNA in Gels. One of the intentions in this study was to monitor the effect of circularization on the Brownian motion of a polymer in a gel network by using the orientation relaxation. In the case of linear DNA, small molecules relax by hindered rotational motion of the whole molecule in gel cavities,[31] whereas for long molecules it occurs through both hindered rotation of polymer segments inside the reptation tube and translational motion out of the tube.[4] The relaxation process is thus capable of conferring information on both rotational and translational Brownian motion. One assumption in the relaxation approach is that the field-oriented initial state is similar to that for the linear control, so that circle relaxation occurs under a similar type of matrix restriction. Our results show that circle relaxation occurs in different parts of the gel, depending on the mode of orientation (impalement or lobster traps). A quantitative comparison with the linear form is therefore difficult, since it is not certain where in the heterogeneous gel the linear form relaxes. When oriented parallel to the field, both pIBI and ΦX174 circles relax somewhat faster than their linear counterparts (ΦX174 is even faster than its linear half) (Figure 13a). Since the larger cavities in polyacrylamide have pore sizes[19] which are comparable to the radii-of-gyration of the DNA, the faster relaxation of the circular forms can be understood (in the spirit of the experiments by Stellwagen[31]) as an effect of their more compact conformation.[20] These results are not in agreement with the relaxation of the parallel component involving translation between different cavities, because then the relaxation would be expected to be slower for the circles due to loop barriers. By contrast, the extremely slow relaxation of the perpendicular component may involve translational motion out of deep traps within or between dense regions, a process which should be considerably slower for the circles due to loop barriers but could also reflect rotational diffusion in very tight cavities from which the linear form can escape more quickly.

Summary

At high fields the degree of orientation of the circles reveals conformations which are significantly nonisotropic, reflecting the strong interaction with the gel matrix which occurs through impalement. The perpendicular orientation at low fields is very weak, but this observation is still important since it reveals a new mechanism of interaction with the gel. The present study shows that an additional method such as LD is essential for studying trapping of DNA, since the information from velocity is limited by the zones being wide or by the complete lack of velocity. LD has the power to resolve the three types of migration in spite of them being present together at the same time, albeit the interpretation is somewhat confounded by the spectroscopic ensemble-averaging. Taken together these observations demonstrate both the strength and weakness of LD: it provides more insight into the migration than velocity because it provides time-resolved conformation data and carries sign information, but the ensemble-averaging means that the net sign may hide a complex conformation distribution.

The present study also shows how electrophoresis of DNA molecules of different topology can be used to probe a gel structure, because linear and circular molecules sample different parts of the gel and because a certain molecular species visits different gel structures at different field strengths.

Acknowledgment. We thank Magn. Bergwall Foundation for financial support and M. Jonsson for fruitful discussions.

References and Notes

(1) Heller, C. *J. Chromatogr. A* **1995**, *698*, 19−31.
(2) Nordén, B.; Elvingson, C.; Jonsson, M.; Åkerman, B. *Q. Rev. Biophys.* **1991**, *24*, 103−164.
(3) Zimm, B. H.; Levene, S. D. *Q. Rev. Biophys.* **1992**, *25*, 171−204.
(4) Åkerman, B. *Electrophoresis* **1996**, *17*, 1027−1036.
(5) Smith, S. B.; Aldridge, P. K.; Callis, J. B. *Science* **1989**, *243*, 203−206.
(6) Long, D.; Viovy, J.-L. *Phys. Rev. E* **1996**, *53*, 803−811.
(7) Åkerman, B. *Phys. Rev. E* **1996**, *54*, 6685−6696.
(8) de Gennes, P.-G. *Scaling concepts in polymer physics*; Cornell University Press: Ithaca, NY, 1979; pp 230−233.
(9) Åkerman, B. *J. Chem. Phys.* **1997**, *106*, 6152−6159.
(10) Mickel, S.; Arena, V.; Bauer, W. *Nucleic Acids Res.* **1977**, *4*, 1465−1482.
(11) Levene, S. D.; Zimm, B. H. *Proc. Natl. Acad. Sci. U.S.A.* **1987**, *84*, 4054−4057.
(12) Serwer, P.; Hayes, S. J. *Electrophoresis* **1987**, *8*, 244−246.
(13) Åkerman, B. *Biophys. J.* **1998**, *74*, 3140−3151.
(14) Larsson, A.; Åkerman, B. *Macromolecules* **1995**, *28*, 4441−4454.
(15) Magnusdottir, S.; Åkerman, B.; Jonsson, M. *J. Phys. Chem.* **1994**, *98*, 2624−2633.
(16) Obukov, S. P.; Rubinstein, M.; Duke, T. *Phys. Rev. Lett.* **1994**, *73*, 1263−1266.
(17) Alon, U.; Mukamel, D. *Phys. Rev. E* **1997**, *55*, 1783−1793.
(18) Hecht, A.-M.; Duplessix, R.; Geissler, E. *Macromolecules* **1985**, *18*, 2167−2173.
(19) Hsu, T.-P.; Cohen, C. *Polymer* **1994**, *25*, 1419−1423.
(20) Vologodskii, A. V.; Cozzarelli, N. R. *Annu. Rev. Biophys. Biomol. Struct.* **1994**, *23*, 609−643.
(21) Bellio, J.; Cooper, J. P.; Hagerman, P. J. *Biochemistry* **1994**, *33*, 1797−1803.
(22) Bloomfield, V. A.; Crothers, D. M.; Tinoco, I. In *Physical Chemistry of Nucleic Acids*; Harper & Row: New York, 1974; pp 159−171.
(23) Jonsson, M.; Åkerman, B.; Norden, B. *Biopolymers* **1988**, *27*, 381−414.
(24) Nordén, B.; Elvingson, C.; Jonsson, M.; Åkerman, B. *Q. Rev. Biophys.* **1991**, *24*, 103−164.
(25) Norden, B.; Kubista, M.; Kurucsev, T. *Q. Rev. Biophys.* **1992**, *25*, 51−170.
(26) Larsson, A.; Åkerman, B.; Jonsson, M. *J. Phys. Chem.* **1996**, *100*, 3252−3263.
(27) Åkerman, B.; Jonsson, M. *J. Phys. Chem.* **1990**, *94*, 3228−3838.
(28) Åkerman, B. *Phys. Rev. E* **1996**, *54*, 6697−6707.
(29) Rhigetti, P. G.; Caglio, S. *Electrophoresis* **1993**, *14*, 573−582.
(30) Liu, M.-K.; Giddings, J. C. *Macromolecules* **1993**, *26*, 3576−3588.
(31) Stellwagen, N. C. *J. Biomol. Struct. Dyn.* **1985**, *3*, 299−314.
(32) Stellwagen, N. C. *Biochemistry* **1988**, *27*, 6417−6424.
(33) Pernodet, N.; Maaloum, M.; Tinland, B. *Electrophoresis* **1997**, *18*, 55−58.
(34) Wijmenga, S. S.; Maxwell, A. *Biopolymers* **1986**, *25*, 2173−2186.
(35) Zivanovic, Y.; Coulet, I.; Prunell, A. *J. Mol. Biol.* **1986**, *192*, 645−660.